Improved polymer thin-film wetting behavior through nanoparticle segregation to interfaces

2007 J. Phys.: Condens. Matter 19 356003

(http://iopscience.iop.org/0953-8984/19/35/356003)

IOP PUBLISHING JOURNAL OF PHYSICS: CONDENSED MATTER

J. Phys.: Condens. Matter **19** (2007) 356003 (16pp) doi:10.1088/0953-8984/19/35/356003

Improved polymer thin-film wetting behavior through nanoparticle segregation to interfaces

R S Krishnan[1], M E Mackay[1], P M Duxbury[2], C J Hawker[3], Suba Asokan[4,5], Michael S Wong[4,5], Rick Goyette[6] and P Thiyagarajan[6]

[1] Department of Chemical Engineering and Materials Science, Michigan State University, East Lansing, MI 48824, USA
[2] Department of Physics and Astronomy, Michigan State University, East Lansing, MI 48824, USA
[3] Materials Research Laboratory, University of California, Santa Barbara, CA 93106, USA
[4] Department of Chemistry, Rice University, Houston, TX 77251, USA
[5] Department of Chemical and Biomolecular Engineering, Rice University, Houston, TX 77251, USA
[6] Intense Pulse Neutron Source, Argonne National Laboratory, Argonne, IL 97251, USA

Received 30 May 2007, in final form 12 July 2007
Published 1 August 2007
Online at stacks.iop.org/JPhysCM/19/356003

Abstract

We report a systematic study of improved wetting behavior for thin polymer films containing nanoparticles, as a function of nanoparticle size and concentration, the energy of the substrate and the dielectric properties of the nanoparticles. An enthalpy matched system consisting of polystyrene nanoparticles in linear polystyrene is used to show that nanoparticles are uniformly distributed in the film after spin coating and drying. However, on annealing the film above its bulk glass transition temperature these nanoparticles segregate strongly to the solid substrate. We find that for a wide range of film thicknesses and nanoparticle sizes, a substrate coverage of nanoparticles of approximately a monolayer is required for dewetting inhibition. Cadmium selenide quantum dots also inhibit dewetting of polystyrene thin films, again when a monolayer is present. Moreover, TEM microscopy images indicate that CdSe quantum dots segregate primarily to the air interface. Theoretical interpretation of these phenomena suggests that gain of linear chain configurational entropy promotes segregation of nanoparticles to the solid substrate, as occurs for polystyrene nanoparticles; however, for CdSe nanoparticles this is offset by surface energy or enthalpic terms which promote segregation of the nanoparticles to the air interface.

(Some figures in this article are in colour only in the electronic version)

1. Introduction

Thin polymer films have numerous applications ranging from microelectronics and sensors to adhesives and bio-medical devices. Yet polymer films made by spincoating or dipcoating are frequently unstable and may dewet upon thermal annealing or solvent exposure due to adverse

surface energies. The thickness of a polymer film plays a very important role in governing its stability [1–5]. For example, a film whose thickness is of the order of a few micrometers may be stable by gravitational forces whereas a thin film (∼100 nm) of the same material is either metastable or unstable on nonwettable substrates. As the film thickness approaches molecular dimensions, intermolecular forces of course become more relevant [3].

Despite the importance of intermolecular forces the macroscopic equilibrium contact angle, which is related to the surface energies in the system, is frequently used to assess the stability of various film/substrate systems at all length scales. However, long range dispersion forces due to induced dipole–induced dipole interactions contribute to the surface energy, yielding an effective interface potential whose strength and magnitude depend on the film thickness, particularly in the thin-film limit. The interface potential can be written as the sum of long range and short range interactions acting across a thin film, yielding the effective surface energies governing film stability [6–10]. However, particularly when nanoparticles are present, entropic terms can also contribute significantly to wetting behavior, as demonstrated in the present study.

The dynamics of thin-film dewetting, as occurs when films are unstable, has also been intensely studied. It has been reported in the literature that thick films (>100 nm) may dewet inorganic substrates by nucleation and hole growth [2, 4] whereas thin films (<100 nm) dewet by spinodal decomposition [11, 12] and/or by film imperfection [13, 14]. Recently, Seemann *et al* [8] reported the dewetting of thin polystyrene (PS) films on silicon oxide substrates and classified them as being unstable due to heterogeneous nucleation or a spinodal process, or both.

Because of its practical and intellectual importance, numerous methods to inhibit dewetting of polymer thin films have been reported in the literature [15–20]. Most of these are based on two approaches: (a) surface treatment of the substrate thereby changing the polymer–surface thermodynamic interaction and/or (b) modifying the polymer. For example, Henn *et al* [20] reported the use of end functional groups with more affinity for the polar substrate as a means of inhibiting the dewetting of thin polystyrene films. A similar study involving modification of the homopolymer by introduction of ionic functionalities was reported by Karim *et al* [18]. Another approach by Yerushalmi and co-workers [19] discussed stabilization of low molecular weight polystyrene thin films by formation of an entangled network between the free chains and long surface-tethered chains. In another study by the same authors, film stability of a polymer melt on a cross-linked network of itself was investigated. It was observed that the melt wets at both low and high cross-link densities but dewets at intermediate densities (autophobicity) [19]. All these approaches have their own advantages and disadvantages depending on the desired application. One disadvantage is that polymer modification to control the wetting behavior of a polymer film leads to a change in the film properties which might be undesirable, for example, in sensor applications [21, 22].

Though at first it appears contrary to the conventional observation of enhanced dewetting in the presence of impurities and other film heterogeneities [13], Barnes *et al* [23] discovered that fullerene nanoparticles inhibit dewetting of thin polymer films on native oxide coated silicon substrates. A similar study by Sharma *et al* [24], reported the improved wetting of thin polystyrene films in the presence of carbon black and colloidal silica particles and, similarly, Mackay *et al* [25] showed that poly(benzyl ether) dendrimers [26] inhibit dewetting of thin polystyrene films.

In an earlier study [27] we demonstrated the stabilizing effect of polystyrene nanoparticles [28] on thin polystyrene films, highlighting the effect of molecular architecture on this process. From neutron reflectivity measurements we showed that the nanoparticles were uniformly distributed in the thin film (of thickness about 40 nm) prior to annealing, yet

Table 1. The weight average molecular weight (M_w), polydispersity index (PDI), polymer radius of gyration (R_g) or nanoparticle radius (a) of the materials used in the present study.

Material	M_w (kDa)	PDI	R_g or a (nm)
Polymers			
PS 5 kDa	5.1	1.07	2.0
PS 19 kDa	19.3	1.07	3.8
PS 75 kDa	75.7	1.17	7.6
PS 211 kDa (20%)[a]	193.0	1.28	12.1
dPS 63 kD[b]	63.5	1.10	6.9
Nanoparticles			
NP 41 kDa	41.0	1.04	2.5
NP 78 kDa	78.0	1.14	3.1
NP 211 kDa	211	1.32	4.3
NP 1.5 MD	1500	1.40	9.0
CdSe quantum dot	34.3	1.01	2.4[c]

[a] Polymer contains 20 mol% units that can be cross-linked via thermal activation.
[b] Polymer is wholly deuterated.
[c] This is the core radius and is surrounded by a steric layer of oleic acid of thickness 2.5 nm.

after annealing above the glass transition temperature they were found to separate to the solid substrate, a silanized silicon wafer. Dewetting was eliminated when the nanoparticles formed a segregated monolayer or above, while below this surface coverage the dewetting dynamics were significantly reduced.

In this paper we explore the effect of polystyrene nanoparticles of different molecular weights (sizes) on the stability of thin polystyrene films of various thicknesses. This extends our previous work [27], where we considered only one nanoparticle size, to a broad range of nanoparticle sizes and we find that larger nanoparticles are more effective at inhibiting dewetting. Moreover, we show that even though CdSe quantum dots segregate primarily to the air interface, they also strongly inhibit dewetting. We argue that segregation of these quantum dots to the film surface is due to the low surface energy of the oleic acid brush on the surface of the organically functionalized CdSe quantum dots. Furthermore, we present results on a variety of substrates indicating that a segregated monolayer or more of nanoparticles, either at the substrate or at the air interface, significantly improves the wetting behavior of thin polymer films.

2. Experiment

Linear polymer standards were obtained from Scientific Polymers and are listed in table 1. The solvents, benzene and toluene, were procured from Sigma-Aldrich Co. The synthesis and characterization of polystyrene nanoparticles and cadmium selenide quantum dots used in this study are reported elsewhere [28–30] and their molecular weights along with their polydispersities are listed in table 1. We do note that the polystyrene nanoparticles and linear precursor polymer that could be cross-linked (PS 211 kDa (20%)) both contained 20 mol% benzylcyclobutane (BCB) with the balance styrene. The BCB could be cross-linked by thermal activation (typically 220–250 °C) and the nanoparticles were prepared by dripping a solution into hot benzyl ether (250 °C) to create single molecule nanoparticles with the possibility of 20 mol% of the monomer units being cross-linked. The quantum dots were prepared exactly as denoted in [29] and were sterically stabilized with an oleic acid layer whose hydrodynamic size was determined by dynamic light scattering (DLS) in toluene (Protein Solutions DLS) and

listed as the steric layer thickness in table 1. The core size was determined by transmission electron microscopy (TEM).

All the polystyrene nanoparticles and polymer standards were checked for any impurities using x-ray photoelectron spectroscopy (XPS) and any contamination was removed by appropriate treatment with hydrofluoric acid [27]. Nanoparticle blend solutions were made by mixing appropriate volumes of stock solutions to obtain solutions containing 1–20 wt% of nanoparticles with respect to the polymer, at an overall concentration ranging from 4–12 mg ml^{-1}. All the solutions were filtered using a 0.2 μm filter before spincoating.

The silicon wafer substrates were used as-received from Wafer World Inc. For both dewetting and neutron reflectivity experiments, the wafers were silanized using Sigmacote®($(SiCl_2C_4H_9)_2O$) (Sigma-Aldrich Co.). In some dewetting experiments, octadecyltrichlorosilane (OTS) ($C_{18}H_{37}Cl_3Si$) (Sigma-Aldrich Co.) was used as the silanizing agent. The silanization was performed by cleaning the wafers in a Piranha bath (70% H_2SO_4 and 30% H_2O_2) for 30 min. The cleaned wafers were then rinsed with copious amounts of Millipore water followed by drying with N_2 and immersion in a 2% silanizing solution in heptane for 2 h. The silanized wafers were rinsed with chloroform and methanol to remove any unreacted silanizing agents [31]. This treatment of silicon wafers resulted in substrates with uniform surface energy. The rms roughnesses of the Sigmacote silanized silicon wafers was below 1 nm as checked with atomic force microscopy (AFM; Pacific Nantechnology NanoR AFM). For some neutron reflectivity experiments, the wafers were used as-received and without any silanization.

Thin films were spun cast, at 5000 rpm for 40 s, from a benzene or a toluene solution onto freshly cleaved mica sheets (Asheville-Schoonmaker Mica Co.). Depending on the concentration of the solution, under these conditions the films produced were approximately 25–80 nm thick as checked with ellipsometry (J A Wollam ellipsometer). The refractive index of the polymer and nanoparticle films as a function of film thickness was also measured using the same ellipsometer. For both the dewetting and neutron reflection experiments, the films were floated onto a clean, deionized water surface and then picked up by the substrate. All the films were dried at 40 °C under vacuum for at least 12 h to ensure complete removal of the entrapped solvent and other potential contaminants. The size of the wafers used for neutron reflectivity experiments was 2 inch in diameter whereas those used for the dewetting experiments were around 1 cm × 1 cm.

All the films were annealed in either air or under a vacuum and the film morphologies after annealing were captured using optical microscopy in the reflection mode. The real-time measurements of the samples were performed by heating them in air under a standard bright field light microscope. The neutron reflection measurements of reflectivity (R) were performed at the POSY2 neutron reflectometer (resolution in Q-space, $\Delta Q/Q \sim 0.05$, Q is the wavevector, $Q = 4\pi \sin(\Theta/2)/\lambda$, Θ is the scattering angle and λ is the neutron wavelength) at Argonne National Laboratory on polymer blend films that were previously annealed at 160–170 °C for times ranging from 2–24 h. The reduced neutron reflectivity data were analyzed using Paratt 32 reflectivity software from HMI Berlin.

TEM samples were prepared by transferring the polymer film onto an epoxy resin (Polybed-812, Polysciences, Warrington, PA, USA) which was then cured at 60 °C for 24 h. The samples were then ultramicrotomed (Power Tome XL, RMC, Tucson, AZ, USA) and imaged using a JEOL 100CX transmission electron microscope.

3. Film stability induced by nanoparticles

Neutron reflectivity measurements have been used to show that the polystyrene nanoparticles are uniformly distributed in the film before annealing, yet after annealing they are found to

Table 2. Values of the fractional coverage (θ) based on the nanoparticle concentration, ϕ, by assuming perfect segregation (using equation (1), and those determined from neutron reflectivity data (θ_{SLD}) using the scattering length density (SLD) and the subsequent nanoparticle volume fraction calculated (ϕ_{SLD}) for the layer next to the substrate (using equation (2)), for blends of nanoparticles NP 78 kDa with dPS 63 kDa.

Nanoparticle wt% (film thickness), figure number	SLD ($10^6 \times$ Å^{-2})	ϕ_{SLD}	θ_{SLD}	θ
5 (45 nm), figure 2(a)	5.66	0.15	0.23	0.36
10 (45 nm), figure 2(a)	4.21	0.44	0.66	0.73
20 (45 nm), figure 2(a)	1.41	1.00	1.50	1.45
10 (27 nm), figure 2(b)	5.16	0.25	0.38	0.44
10 (39 nm), figure 2(b)	4.72	0.34	0.51	0.63
10 (77 nm), figure 2(b)	1.88	0.91	1.37	1.24

separate to the solid substrate and to retard the dewetting kinetics of the linear polymer [27]. A crude estimate of the fractional aerial coverage (θ) of the nanoparticles at the substrate, based on a simple mass balance, is given by

$$\theta = (h/2a) \times \phi \tag{1}$$

where h is the film thickness, a the nanoparticle radius and ϕ the bulk nanoparticle volume fraction. $\theta \approx 1$ corresponds to a dense packed monolayer of nanoparticles at the substrate. It was shown in previous work [27], and is further demonstrated here, that dewetting is severely retarded for nanoparticle volume fractions corresponding to a segregated nanoparticle monolayer or more. Below we extract θ from analysis of neutron reflectivity data and we correlate the value of θ with the degree to which dewetting is inhibited.

It is evident from equation (1) that if the nanoparticles segregate to the substrate, then θ can be controlled by either varying the thickness of the film or the bulk nanoparticle volume fraction. This control is illustrated by analysis of neutron reflection measurements from thin polymer films (thickness 27–77 nm) containing 5–20 wt% protonated nanoparticles (weight average molecular weight $\equiv M_w = 78$ kDa) with deuterated linear polystyrene (dPS, $M_w = 63$ kDa). Neutron reflectivity profiles for nanoparticle blend films containing 5–20 wt% nanoparticles and thickness approximately 45 nm are given in figure 1(a), where the profiles are offset by a factor of 10 for clarity. All the films in this figure were annealed in air for 24 h at a temperature of 160 °C, except the 5% blend for which annealing was restricted to 2 h to limit dewetting. The reflectivity profiles in figure 1(b) correspond to nanoparticle blend films with one concentration, approximately 10 wt%, of nanoparticles; however, the film thickness was varied from 27 to 77 nm. These films were annealed in air for 6 h at 160 °C.

Fits to the neutron reflectivity data of figures 1(a) and (b) were based on a two-layer model, where the top layer is composed of pure (deuterated) linear polymer (dPS 63 kDa) and the bottom layer consists of both the linear polymer and nanoparticles. For example, for the 39 nm thick film of a 10 wt% blend shown in figure 1(b), one finds the scattering length density (SLD) of the layer next to the substrate to be 4.72×10^{-6} Å^{-2} whereas the top layer has an SLD of 6.42×10^{-6} Å^{-2} (see table 2). In fitting this reflectivity profile, the pure polymer–nanoparticle-rich layer interface roughness was found to be 4 nm and the nanoparticle layer thickness was 6.2 nm. Of course, the roughness relative to the layer thickness is large and so may not have physical significance. The resolution of the Q-vector ($\Delta Q/Q$) for the instrument was also employed as a fitting parameter and was found to be approximately 0.03, a reasonable value.

A test of alternative models is presented in figure 1(c) for the case of the 39 nm thick film containing 10 wt% nanoparticles, where a plot of RQ^4 versus Q for the data and various

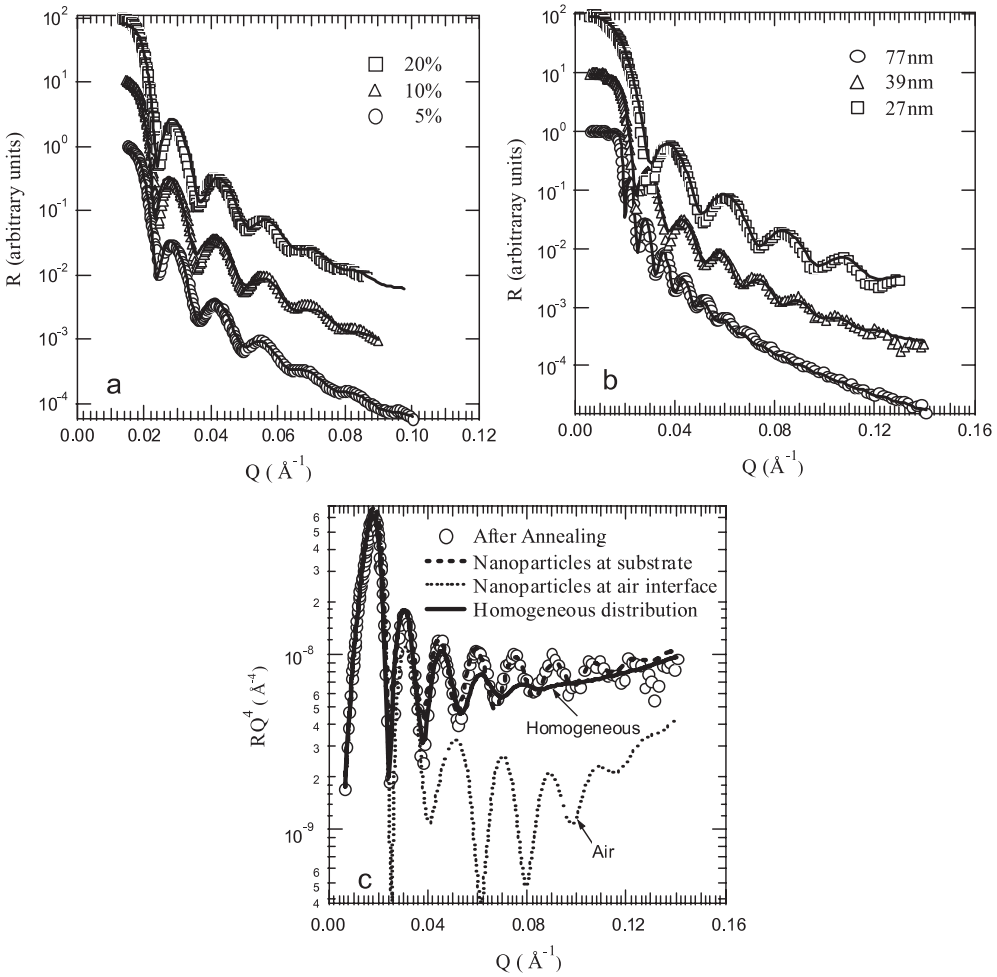

Figure 1. Reflectivity versus wavevector for nanoparticle blends of deuterated linear polystyrene, dPS 63 kDa, and polystyrene nanoparticles (NP, 78 kDa). The films were annealed in air at 160 °C. The data in (a) and (b) are offset by a factor of 10 for clarity. (a) Data for nanoparticle concentrations 5, 10 and 20 wt% at fixed film thickness, approximately 45 nm. The 10 and 20 wt% films were annealed for 24 h, while the 5 wt% film was annealed for 2 h. (b) Data for fixed nanoparticle concentration, 10 wt%, for film thicknesses 27, 39 and 77 nm, after annealing for 6 h. (c) Reflectivity multiplied by reflectance wavevector to the fourth power (RQ^4) versus Q using the 39 nm thick film data of figure 2(b), and a comparison of fits to three different models placing the nanoparticles at the substrate or air interface or homogeneously distributed throughout the film (see text for details).

modeling results are presented. This type of plot is useful when considering sharp interfaces and R should decay as Q^{-4} when they are present. Three models are compared to the data in this figure, firstly a model where complete phase segregation to the substrate occurs as discussed above, secondly, a case of homogeneous distribution of nanoparticles in the film and thirdly, a case where the nanoparticles segregate to the air interface. Clearly, the latter model does not predict the observed reflectivity profile. The case of homogeneous distribution shows little difference from the observed reflectivity at low Q but does not represent the data at high Q. Only the case of nanoparticles separating to the hard substrate gives a satisfactory

agreement with the observed reflectivity at both low and high values of the wavevector. In all cases in figure 1, a critical wavevector (Q_c) which is approximately 0.017 ± 0.001 Å^{-1}; denotes the wavevector where the reflectivity falls rapidly from 1. If the nanoparticles migrated to the air interface the critical wavevector would have moved to lower values, since the nanoparticles have a lower SLD than the bulk polymer, which is not the case here.

From the SLD of the bottom layer, the volume fraction of the nanoparticles can be estimated as described below. In our previous studies [32, 33], we have shown that the nanoparticles collapse to a volume given by their molecular weight and the density of bulk polystyrene, making the nanoparticle volume and weight fraction equivalent. In the case of the 39 nm thick film in figure 1(c), the nanoparticle layer thickness next to the substrate is approximately given by its diameter (∼6.2 nm). By knowing the polymer and nanoparticle SLD, 6.42×10^{-6} Å^{-2} and 1.41×10^{-6} Å^{-2}, respectively, one is able to determine the nanoparticle volume fraction (ϕ_{SLD}) in the layer which for the above example is 0.34.

Now one can relate this volume fraction to the fractional arial coverage, θ_{SLD}, by assuming a regular array of nanoparticles at the substrate. Assuming a hexagonal array of spherical nanoparticles of radius a, where Δ is the half-gap between the particles for sub-monolayer coverages, we have $\phi_{SLD} = (\pi/3\sqrt{3})(a^2/(\Delta + a)^2)$. The aerial coverage is the projected area, so that $\theta_{SLD} = (\pi/2\sqrt{3})(a^2/(\Delta + a)^2)$, and

$$\theta_{SLD}/\phi_{SLD} = 3/2. \tag{2}$$

Note that the assumed packing geometry does not change the aerial coverage estimate which appears valid for any packing. Comparison of the experimental results for θ_{SLD} with those expected from perfect segregation (table 2) shows good agreement. Error estimates of these values are difficult to quantify and are primarily due to uncertainties in the parameters extracted from fitting the neutron reflectivity data.

The effect of varying the fractional surface coverage on the dewetting behavior of thin films on a Sigmacote surface is illustrated in figure 2. It is observed that at fractional coverages θ less than a monolayer dewetting occurs; however, at coverages greater than a monolayer dewetting is eliminated in agreement with our previous study with a different nanoparticle size [27]. The effect of substrate surface energy on dewetting behavior is considered by a comparison of dewetting behavior of linear polystyrene on a Sigmacote surface, which has a surface energy 28.5 ± 4.9 mJ m^{-2} at room temperature, as compared to a OTS surface, which has a lower surface energy (≈24 mJ m^{-2}), in figure 3. The films in this figure were spuncast on a mica surface, floated onto a silanized (Sigmacote or OTS) silicon substrate and then annealed in air. In the case of OTS, the alkane chain is 18 carbon atoms long (∼4 nm thick layer) while the alkane chains of a Sigmacote surface contain only four carbon atoms (∼1 nm thick layer) [31].

More rapid dewetting occurs for OTS substrates (compare figures 3(a) and (e)); we quantify this in figure 4 before returning to discussion of figure 3, where we present the rate of hole growth for linear polystyrene films (about 45 nm thick) at 160 °C as a function of polystyrene molecular weight and substrate surface energy. In all cases the hole radius grows with time as $R \sim t^{2/3}$, implying slip [34–36], to show dewetting occurs on the timescale of minutes. The dewetting velocity for polymers is inversely related to their viscosity which increases with molecular weight, as can be seen in the data for PS on Sigmacote. The rate of hole growth for PS 75 kDa on an OTS functionalized substrate is significantly faster than on a Sigmacote substrate, due to the lower surface energy of the OTS substrate [35]. Thus, as expected, a lower surface energy substrate leads to more rapid dewetting of thin polymer films.

The optical microscopy images of figure 3 illustrate the combined effects of substrate surface energy and nanoparticle size on dewetting behavior for linear polystyrene/polystyrene nanoparticle films with a constant thickness of ∼50 nm. As discussed above, pure polymer

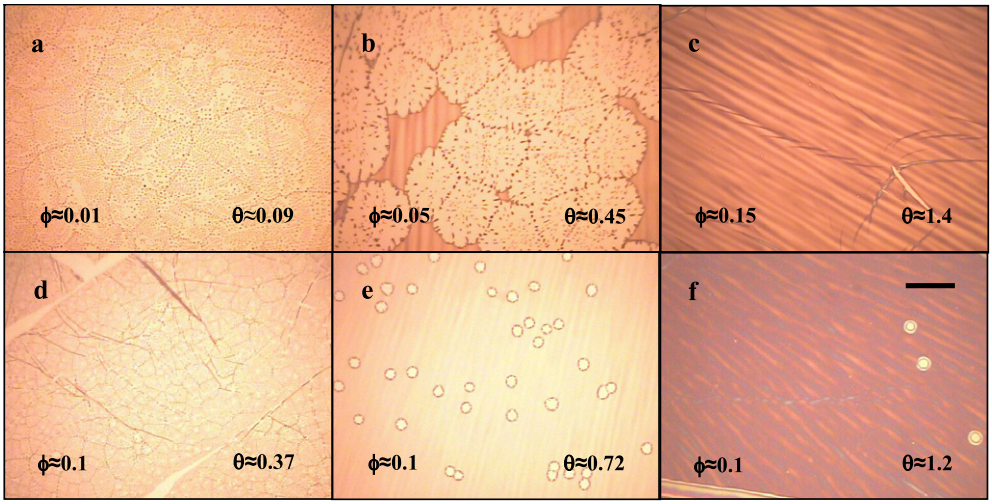

Figure 2. Optical micrographs of blends of linear polymer (PS 75 kDa) with PS nanoparticles (NP 78 kDa) after annealing the films for 24 h in vacuum at 160 °C on a silanized Sigmacote® substrate. In (a)–(c) the nanoparticle fractional areal coverage (θ) is varied by changing the bulk nanoparticle concentration (ϕ) at a constant thickness of 56 nm; the volume fractions are 0.01 (a), 0.05 (b) and 0.15 (c). In (d)–(f) θ is varied by changing the overall film thickness at a fixed nanoparticle concentration of 10 wt%. The film thicknesses are: 23 nm (d), 45 nm (e) and 76 nm (f). In both cases a fractional coverage of a monolayer is needed to severely retard the dewetting of the linear polymer as shown by the film stability in (c) and (f). The length of the scale bar is 200 μm.

films dewet at times of the order of a few minutes while polymer films containing nanoparticles exhibit significantly increased stability, as demonstrated in figure 3. The nanoparticle surface coverage is just above a monolayer in all cases and the films were annealed at 170 °C under a vacuum. For the smallest nanoparticle, dewetting occurs on both Sigmacote and OTS substrates (figures 4(a), (e), (i)). Nanoparticles of size 6.2 nm (figures 4(b), (f), (j)) are stable after 1 day on Sigmacote, but begin to dewet in 1 day and completely dewet from OTS substrates after 5 days (figures 4(f) and (j)). The larger nanoparticles yield films that are stable after 5 days on OTS substrates (figures 4(k) and (l)) and are most likely similarly stable on Sigmacote surface after 5 days because of its higher surface energy. Moreover, we noticed that for each of the nanoparticle blend films in figure 3, increasing the nanoparticle concentration further above a monolayer imparts more stability to the film against dewetting. These data support and extend the results of [27] where 5.0 nm diameter nanoparticle ($M_w = 41$ kDa) blend films were stable on the Sigmacote substrate at concentrations above a monolayer.

4. Theoretical rationalization

In polystyrene nanoparticle/linear polystyrene systems, segregation of the nanoparticles to the substrate is driven by an entropy gain for the entire system [37], a mechanism similar to that arising when low molecular weight polymers are mixed with high molecular weight polymers of the same composition [38]. A simple argument can be made [37] to justify this segregation by noting that the monomer units in a linear polymer will gain $\alpha k_B T[a/\sigma]^3$ of entropy when they move from the solid substrate and push a nanoparticle down. Here α is the number of degrees of freedom gained by a given monomer unit, k_B is the Boltzmann constant, T is temperature and σ is the size of a monomer unit. The nanoparticle itself will lose $\sim k_B T$

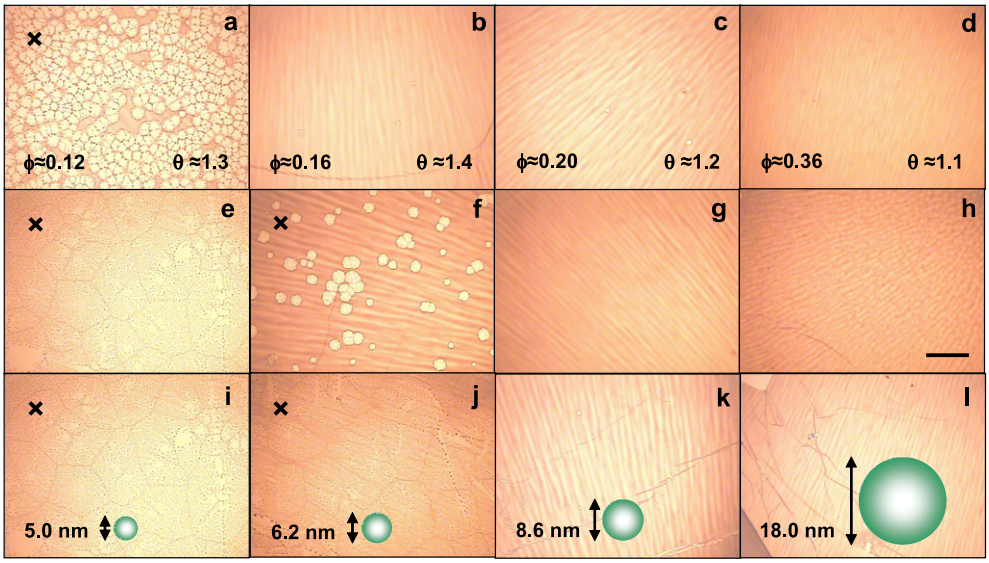

Figure 3. Optical micrographs of blends of linear polymer (PS 75 kDa) with polystyrene nanoparticles of four different molecular weights: 41 kDa (diameter ≈5.0 nm), 78 kDa (6.2 nm), 211 kDa (8.6 nm) and 1.5 MDa (diameter 18.0 nm). A scaled representation of each nanoparticle is given in the bottom row of photographs with each column representing a film containing these nanoparticles at the volume fraction (ϕ) given in the top row. These conditions result in a monolayer or above of nanoparticles at the solid substrate ($\theta \approx 1$) as shown in the top figures. All the films have an approximately constant thickness of 50 ± 7.2 nm. The top row ((a)–(d)) is the result of annealing the films at 170 °C under vacuum for 1 day where the substrate was a silicon wafer coated with Sigmacote. The middle row ((e)–(h)) is the result under the same annealing conditions except the substrate was an OTS coated wafer. The bottom row ((i)–(l)) shows the same samples with an OTS coated wafer except they have been aged for a longer time of 5 days. The × in the upper left-hand corner highlights the fact that this system has partially or fully dewetted. The length of the scale bar is 200 μm.

worth of translational entropy while segregation from the blend costs $\varepsilon[a/\sigma]^2$ of mixing free energy [30] to account for monomer interactions with the nanoparticle surface, ε is of order 0.1–$1k_BT$ for dispersion forces. A simple balance between these thermodynamic components shows that $\alpha[a/\sigma]^3 > 1 + [\varepsilon/k_BT]\,[a/\sigma]^2$ for segregation, requiring that a monomer unit in a linear chain near the substrate must gain 0.01–0.1 degrees of freedom due to constraint release when nanoparticle segregation occurs. It is expected, however, that α is of the order of 1, demonstrating that an entropy based mechanism is certainly capable of driving segregation, as is consistent with nanoparticle segregation observed in self-consistent field calculations of nanoparticle segregation in blends [39] and also with density functional calculations we are currently performing in our group.

The wetting stability of thin polymer films depends on long range van der Waals forces acting across the film [40], as discussed above. Though complete assessment of these forces is based on sophisticated electromagnetic theories [3, 41], a pairwise additive theory introduced by Hamaker explains why polystyrene dewets from silanized silicon wafers [8, 40]. Multilayer geometries are discussed thoroughly in the recent book by Parsegian [41] and in work on lubrication of magnetic read heads [42]. So we consider a segregated layer of polystyrene nanoparticles to act as a buffer layer attenuating the destabilizing effect of van der Waals forces of the silanized silicon wafers used in our studies. Since, in this system, the nanoparticles are

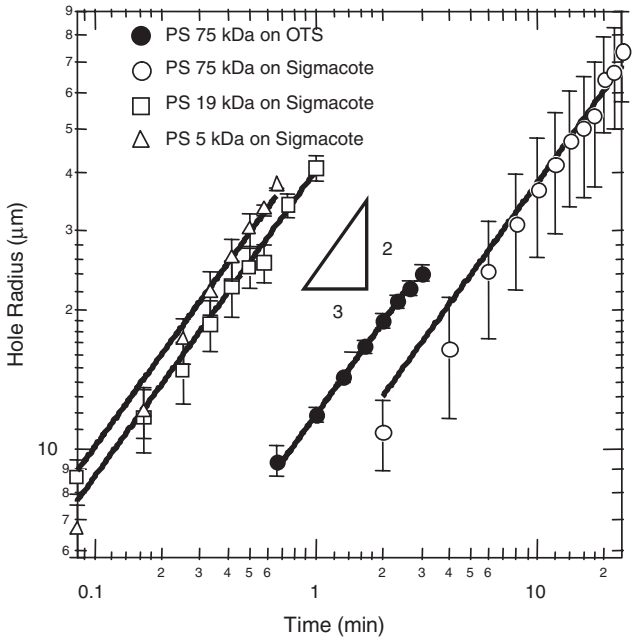

Figure 4. Hole radius versus time during annealing in air at 160 °C for pure linear PS 75 kDa, PS 19 kDa and PS 5 kDa along with power law fits on two different silanized substrates. In all cases the dewetting rate follows a power law of 2/3 implying slip. Use of OTS compared to Sigmacote as the silanizing agent increases the rate of dewetting for the pure PS 75 kDa films. The film thickness in all cases is approximately 45 nm.

chemically similar to the bulk linear polymer, it is apparent that molecular architecture plays an important role in retarding dewetting and is promoted by the self-assembly process described above [37].

We checked that the polystyrene nanoparticles used in this study do in fact have a similar refractive index, and hence similar dielectric or van der Waals forces, to that of linear polystyrene. Due to their nanoparticle morphology [32, 43], cross-linking within the nanoparticle or perhaps interface effects [44] this quantity may have been quite different. The measured refractive index of both linear polystyrene and nanoparticle films as a function of film thickness is shown in figure 5 and it is found that they have almost the same refractive index for all film thicknesses, though deviations from bulk behavior in both cases develop at film thicknesses less than about 20 nm. Our studies of wetting phenomena are in the regime greater than 20 nm where these deviations are not significant, and so the reduced refractive index is not considered significant to our study. We admit the segregated nanoparticle layer is of the order 5–10 nm thick; however, it is expected that the polymer layer above it acts as a super-layer to minimize this effect as we have proved through ellipsometry of aged films.

Analysis of the effect of nanoparticle segregation on dewetting inhibition combines the analysis of van der Waals forces and the stabilizing effects of nanoparticles. In the case of polystyrene nanoparticles in polystyrene melts, we consider a six-layer system consisting of Si/SiO_2/Brush (Sigmacote or OTS)/NP/PS/air. However the NP and PS have essentially the same dielectric behaviors, as discussed above, and from the viewpoint of van der Waals forces can be treated as a single layer. Using a five-layer van der Waals theory within the non-retarded approximation, which is believed to be reasonable for films less than 100 nm thick (though

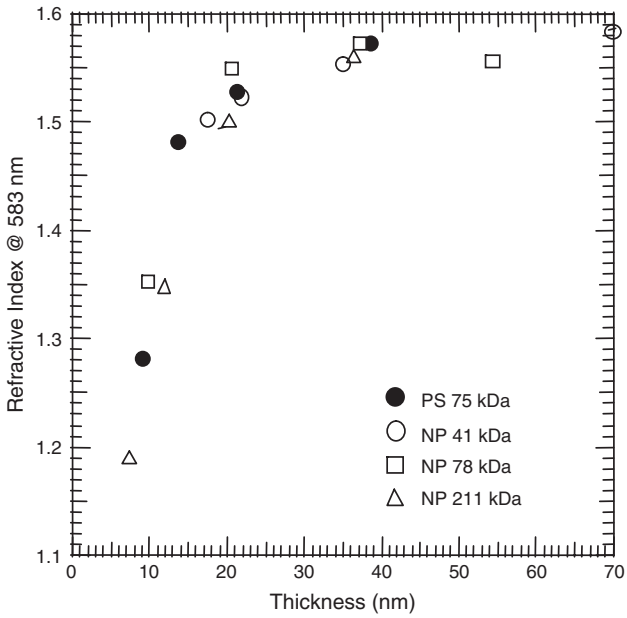

Figure 5. Refractive index at 583 nm as a function of film thickness for linear polystyrene, PS 75 kDa ($2R_g \approx 15$ nm) and polystyrene nanoparticles: NP 41 kDa ($2a \approx 5$ nm), NP 78 kDa ($2a \approx 6.2$ nm) and NP 211 kDa ($2a \approx 8.6$ nm).

see [10]), the PS/air interface potential (V_d) has the general form

$$V_d = \frac{A_1}{12\pi(d_{SiO_2} + d_{brush} + h)^2} + \frac{A_2}{12\pi(d_{brush} + h)^2} - \frac{A_3}{12\pi h^2} + V_R(h) \qquad (3)$$

where d_{SiO_2} is the oxide thickness, d_{brush} is the thickness of the alkane brush (i.e. OTS or Sigmacote) and $h = d_{NP} + d_{PS}$ is the sum of the nanoparticle layer thickness (d_{NP}) and the thickness of the thin linear polymer film (d_{PS}). The Hamaker constants, A_1, A_2, A_3, may be determined in several ways, as discussed below, and $V_R(h)$ is the repulsive potential. In the absence of nanoparticles, the repulsive potential is empirically determined and is usually taken to be of the form c/h^8 [8, 40] with c assumed equal to 0.05 zJ nm^6 (zJ = zeptoJoule). However, in the presence of nanoparticles, it is energetically unfavorable to break up the segregated nanoparticle layer, leading to a repulsive potential with a length scale proportional to the segregated nanoparticle layer thickness, and so we assume that a repulsive potential of the form

$$V_R(h) = v_r \mathrm{Exp}[-a_r h/d_{NP}] + c/h^8 \qquad (4)$$

is appropriate. In this expression v_r determines the strength of the repulsion due to nanoparticle segregation while d_{NP}/a_r is the length scale over which this repulsion is significant. The disassembly energy, v_r, is the energy per unit area required to break up the segregated nanoparticle layer and is taken as $\alpha k_B T d_{NP}/\pi r^2 L_k$ where r is the monomer size and L_k is the Kuhn segment size (1.59 nm [45]). This expression is a product of the entropy gain per released monomer $\alpha k_B T$, discussed earlier, and an estimate of the number of monomers released per unit area which increases with the nanoparticle layer thicknesses for small enough values of d_{NP}. The nanoparticle thickness over which constraint release is possible is uncertain, but we expect it to be no larger than the radius of gyration of the linear polymer chains in the melt and it may

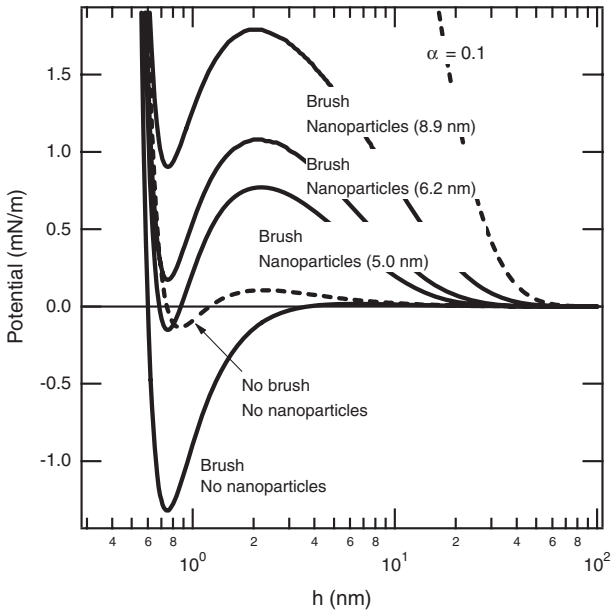

Figure 6. Interface potential as a function of film thickness for various systems using equations (3) and (4) and parameters discussed in the text. When only the native oxide is present on the silicon wafer (no brush, no nanoparticles) the system is metastable while silanizing the surface (brush, no nanoparticles) makes the system unstable and it will dewet to an equilibrium sub-nanometer thick film. A monolayer of nanoparticles, of diameter 5.0, 6.2 or 8.9 nm, can create a metastable layer that is more and more 'stable' as the nanoparticle size is increased (brush, nanoparticles (5.0 nm), etc). Increasing the α parameter from 0.02 to 0.1 for the 8.9 nm diameter nanoparticles produces a fully stable film (curve labeled $\alpha = 0.1$).

be as small as the coherence length of the polymer melt. Density functional theory calculations may resolve this issue and also provide an improved estimate of v_r [48].

Estimates of the Hamaker constant values are possible by noting that in the limit $d_{\text{brush}} = 0$, the expression (3) must reduce to that used by Seeman *et al* [8, 40] in their studies of dewetting of polystyrene from oxidized Si substrates. They found estimates of the Hamaker constants for the trilayers Si/PS/air ($A_{\text{Si}} = -130$ zJ), and SiO_2/PS/air ($A_{\text{SiO}} = 22$ zJ), and used them to find estimates of the Hamaker constants for the four-layer system Si/SiO_2/PS/air. For small brush thickness, we reproduce those values through the relations $A_1 = A_{\text{SiO}} - A_{\text{Si}}$, $A_2 = A_{\text{brush}} - A_{\text{SiO}}$ and $A_3 = A_{\text{brush}}$. Lifshitz theory [3] implies that the dependence of trilayer Hamaker constants is quadratic in the refractive index differences, having the form $\sim[n_1^2 - n_3^2] \times [n_2^2 - n_3^2]$ for medium 3 between 1 and 2. Noting that the refractive indices of polystyrene, SiO and the brush are, respectively, 1.59, 1.5 and 1.4, the value of A_{brush} is approximately twice as large in magnitude as A_{SiO}. This yields the estimates $A_1 \sim 150$ zJ, $A_2 \sim 22$ zJ and $A_3 \sim 44$ zJ which are rough estimates for a variety of reasons, including deviations from ideal planar geometries and neglect of the non-ideal nature of interfaces. Moreover, theoretical calculations also differ significantly from the experimentally determined values [8, 40], particularly for the case of SiO_2.

Nevertheless, the expressions (3) and (4) provide a clear picture of the destabilization induced by the brush layer and the stabilizing effect of a segregated nanoparticle layer on polystyrene film wetting, as illustrated in figure 6. The oxide layer thickness (d_{SiO}) in this example is 2 nm which leads to destabilization of polystyrene thin films [8, 40]. We have

found in our experiments that a metastable state is present, since at times the film will dewet on this substrate, though in other samples it can remain stable in agreement with the theoretical calculation. The addition of a brush ($d_{\text{brush}} = 2$ nm) leads to stronger destabilization as evidenced by the bottom trace in figure 6, the addition of nanoparticles stabilizes the films, even in the presence of a brush (see the top trace in figure 6). The dispersion force parameters used in these figures are consistent with those used by Seeman *et al*, as is the value of c that characterizes the strength of the c/h^8 repulsive term in equation (4).

Two parameters characterize the new exponential repulsive term in equation (4) and are important to the stability of thin polystyrene films. The length scale over which the segregated nanoparticle layer is effective is taken to be equal to the thickness of the nanoparticle layer, as used in figure 6, where we assume $a_{\text{r}} = 1$. If the nanoparticle layer is diffuse or the nanoparticles are not fully segregated this parameter may be either increased or decreased. Though this length scale certainly affects the theory, the most important parameter is the disassembly energy, v_{r}. If this energy is small, the nanoparticle layer has no effect on the stability of thin films, while if it is large the films are very strongly stabilized. The disassembly energy used in figure 6 is of the order 1 zJ nm^{-2} which is assumed relatively small by taking $\alpha = 0.02$, in the range of energies discussed above, and can be related to the entropy gain on nanoparticle segregation. From this, one can also argue that the larger nanoparticles (8.9 nm) yield larger activation barriers, as illustrated in figure 6. Finally, increasing α to 0.1 or that a monomer unit next to the wall gains 0.1 degrees of freedom by pushing the nanoparticle down yields a film that is very stable, indicating that it is possible to make a polymeric coating even when adverse wetting conditions are present, i.e. in the presence of an alkane brush layer.

In cases where the nanoparticle filled polymer films are unstable, the dewetting dynamics is significantly slower, both in requiring a long nucleation time and exhibiting a reduced hole growth rate. It is evident that metastability is induced by segregated nanoparticle layers (see figure 6) and the observed (slow) dewetting of lower molecular weight PS nanoparticle filled PS films may be due to jamming [46] of nanoparticles during flow. Moreover, we have found [32] that the lowest molecular weight nanoparticles (PS 41 kDa) do not have an apparent yield stress, at least not one that we could measure, in the bulk which could allow them to flow and hence for dewetting to eventually occur which appears to be the case for the results shown in figure 3.

5. Generalization

The stabilizing effect of nanoparticles on thin polymer film wetting is a more general phenomenon and may occur when nanoparticles segregate to the air interface, as we demonstrate by using a blend of linear polystyrene and cadmium selenide quantum dots (diameter ≈4.7 nm). This blend exemplifies a system where dispersion forces and surface energy compete with entropy in determining nanoparticle segregation. A TEM micrograph of the cross-section of a four-layer film of PS 211 kDa is shown in figure 7(a). This multilayer film was fabricated using cross-linkable linear polystyrene of molecular weight 211 kDa. The first layer of the film contained a blend of this polystyrene (PS 211 kDa (20%), table 1) and 22 wt% ($\phi = 0.046$, $\theta \approx 0.75$) quantum dots, and after spincasting it was annealed for 30 min at 230 °C under vacuum. This annealing enables both segregation of the nanoparticles and cross-linking of the linear PS providing a solid substrate for the second layer. The second layer was spincast using pure cross-linkable polystyrene and then cross-linked in a similar manner by heating the sample [37]. The third and fourth layers were fabricated using a similar procedure to that used for the first layer through successive spincoating, assembling and cross-linking. It is evident from this multilayer material that the quantum dots segregate to both the solid substrate and to the air interface in the first layer, but mostly to the air interface, and segregate almost

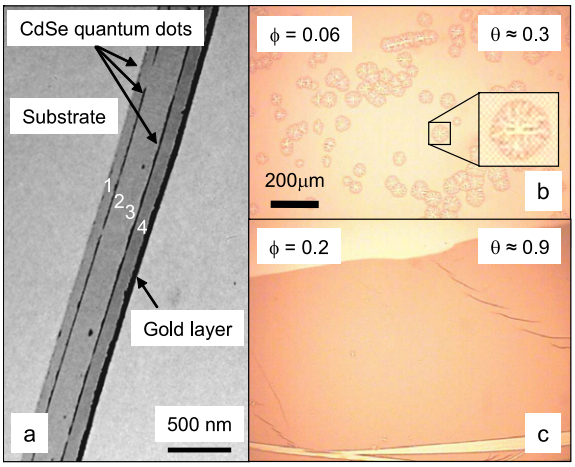

Figure 7. (a) Cross-sectional TEM micrograph of four PS 211 kDa layers where some contain CdSe quantum dots as described in the text. Layer 2 does not have any quantum dots in it while layer 3 does and in this layer they predominantly assemble at the air interface when the polymer film is heated. Each polymer layer is approximately 75 nm thick and the gold layer was sputtered on the layered assembly as a focussing aid. (b) A sub-monolayer coverage of quantum dots on a polystyrene film does not inhibit dewetting ($\phi = 0.06$, $\theta \approx 0.3$) after aging for 24 h at 180 °C on an OTS coated silicon wafer; however, near a monolayer it does ($\phi = 0.2$, $\theta \approx 0.9$) as shown in (c). Note how the dewetting pattern in (b) (see inset) is different from the patterns displayed in figures 2 or 3.

exclusively to the air interface in the third layer, remember the second layer has no quantum dots in it.

The hydrocarbon coating (oleic acid) capping the quantum dots has a lower surface energy relative to the polystyrene matrix and this provides a driving force for their segregation to the air interface. Of course, due to the presence of a substrate another entropic force is present which pushes the nanoparticles to the substrate; hence competition occurs. We find though that CdSe nanoparticles form a stable wetting layer at the air interface and stabilize the whole film for layers 3 and 4 in the figure while layer 1 has most of the nanoparticles at the air interface.

The ability of quantum dots to promote wetting of polymer thin films on OTS substrates is demonstrated in figures 7(b) and (c), where it is seen that again a monolayer coverage strongly enhances wetting of polystyrene on OTS. The sample was aged for 24 h at 180 °C, conditions which are severe enough to promote dewetting of a pure polymer film in minutes. Thus, whether the nanoparticles are at the solid substrate or at the air interface wetting is promoted which can be justified by equation (3) although uncertainties in estimating coefficients can produce multiple results and conclusions.

Regardless, the sterically stabilized quantum dots promote wetting when a monolayer or above is present, yet below this coverage (figure 7(b)) unusual dewetting patterns are present compared to those in figures 2 and 3. Here it is clear that the system dewets by another mechanism with patterns similar to those observed during solvent annealing [22, 47] perhaps due to their position at the air interface.

6. Conclusion

We have presented a systematic study of the effect of nanoparticles on the dewetting behavior and stability of polymer thin films. Two different types of nanoparticles were used to inhibit

dewetting, polystyrene nanoparticles and CdSe quantum dots. Neutron reflectivity data provide convincing evidence that polystyrene nanoparticles segregate to the substrate on annealing, while TEM images show that CdSe quantum dots predominantly segregate to the air surface. Though entropic gain drives the PS nanoparticles to the substrate, this is offset in the CdSe case by the low surface energy of the oleic acid layer on the quantum dot surfaces, leading to the observed surface segregation of these nanoparticles.

Higher molecular weight polystyrene nanoparticles strongly enhance the wetting behavior of polystyrene thin films; moreover for all polystyrene nanoparticle sizes a substrate coverage of a monolayer is essential to provide the strongest inhibition of dewetting. Neutron reflectivity data demonstrate that the nanoparticle substrate coverage can be changed by varying the thickness of the film and/or the bulk volume fraction of nanoparticles, providing two avenues for the control of dewetting; this is also true for the quantum dot system.

The segregation of nanoparticles to interfaces is determined by the interplay between entropic gain, which is dominant in the case of polystyrene nanoparticles, and enthalpic terms which dominate in the case of CdSe nanoparticles. Wetting behavior is most simply understood in terms of an interplay between long range dispersion forces and a short range repulsion due to nanoparticle segregation, yet a complete theoretical description of both nanoparticle segregation and thin-film wetting is lacking and remains a major challenge to theorists in the field. Nevertheless the phenomenological repulsive term introduced in equation (4) can be used to suggest that strongly segregating nanoparticle/polymer systems provide the largest values of the segregation energy, v_r, and lead to greater improvement of wetting behavior. However, this tendency must be balanced by the fact that segregation of nanoparticles in the body of the polymer film is deleterious, so that careful tuning of the tendency to segregation is necessary to optimize the improvement in wetting behavior though nanoparticle segregation to interfaces.

Acknowledgments

This research was primarily supported by DE-FG02-05ER46211 and through NSF CTS-0400840, NSF NIRT-0210247, NSF-CTS-0417640, NSF NIRT-0506309, NSF DMR-0520415, DE-FG02-90ER45418, ARO W911NF-05-1-0357. Support by the US Department of Energy, BES-Materials Science, under contract no. W-31-109-ENG-38 to the University of Chicago is greatly appreciated.

References

[1] Redon C, BrochardWyart F and Rondelez F 1991 *Phys. Rev. Lett.* **66** 715–8
[2] Reiter G 1992 *Phys. Rev. Lett.* **68** 75–8
[3] Israelachvili J N 1992 *Intermolecular and Surface Forces* (London: Academic)
[4] Sharma A and Reiter G 1996 *J. Colloid Interface Sci.* **178** 383–99
[5] Muller-Buschbaum P 2003 *J. Phys.: Condens. Matter* **15** R1549–82
[6] Tidswell I M, Rabedeau T A, Pershan P S and Kosowsky S D 1991 *Phys. Rev. Lett.* **66** 2108–11
[7] Reiter G, Sharma A, Casoli A, David M O, Khanna R and Auroy P 1999 *Langmuir* **15** 2551–8
[8] Seemann R, Herminghaus S and Jacobs K 2001 *J. Phys.: Condens. Matter* **13** 4925–38
[9] Seemann R, Herminghaus S, Neto C, Schlagowski S, Podzimek D, Konrad R, Mantz H and Jacobs K 2005 *J. Phys.: Condens. Matter* **17** S267–90
[10] Zhao H P, Wang Y J and Tsui O K C 2005 *Langmuir* **21** 5817–24
[11] Vrij A 1966 *Discuss. Faraday Soc.* **42** 23–33
[12] Reiter G 1993 *Langmuir* **9** 1344–51
[13] Stange T G, Evans D F and Hendrickson W A 1997 *Langmuir* **13** 4459–65
[14] Jacobs K, Herminghaus S and Mecke K R 1998 *Langmuir* **14** 965–9
[15] Orlicki J A, Moore J S, Sendijarevic I and McHugh A J 2002 *Langmuir* **18** 9985–9

[16] Wunnicke O, Lorenz-Haas C, Muller-Buschbaum P, Leiner V and Stamm M 2002 *Appl. Phys. Mater. Sci. Proc.* **74** S445–7
[17] Yuan C G, Meng O Y and Koberstein J T 1999 *Macromolecules* **32** 2329–33
[18] Feng Y, Karim A, Weiss R A, Douglas J F and Han C C 1998 *Macromolecules* **31** 484–93
[19] Kerle T, YerushalmiRozen R and Klein J 1997 *Europhys. Lett.* **38** 207–12
[20] Henn G, Bucknall D G, Stamm M, Vanhoorne P and Jerome R 1996 *Macromolecules* **29** 4305–13
[21] Grate J W and McGill R A 1995 *Anal. Chem.* **67** 4015–9
[22] Holmes M A, Mackay M E and Giunta R K 2007 *J. Nanopart. Res.* **9** 753–63
[23] Barnes K A, Karim A, Douglas J F, Nakatani A I, Gruell H and Amis E J 2000 *Macromolecules* **33** 4177–85
[24] Sharma S, Rafailovich M H, Peiffer D and Sokolov J 2001 *Nano Lett.* **1** 511–4
[25] Mackay M E, Hong Y, Jeong M, Hong S, Russell T P, Hawker C J, Vestberg R and Douglas J F 2002 *Langmuir* **18** 1877–82
[26] Hawker C J and Frechet J M J 1990 *J. Am. Chem. Soc.* **112** 7638–47
[27] Krishnan R S, Mackay M E, Hawker C J and Van Horn B 2005 *Langmuir* **21** 5770–6
[28] Harth E, Van Horn B, Lee V Y, Germack D S, Gonzales C P, Miller R D and Hawker C J 2002 *J. Am. Chem. Soc.* **124** 8653–60
[29] Asokan S, Krueger K M, Alkhawaldeh A, Carreon A R, Mu Z Z, Colvin V L, Mantzaris N V and Wong M S 2005 *Nanotechnology* **16** 2000–11
[30] Mackay M E, Tuteja A, Duxbury P M, Hawker C J, Van Horn B, Guan Z B, Chen G H and Krishnan R S 2006 *Science* **311** 1740–3
[31] Brzoska J B, Benazouz I and Rondelez F 1994 *Langmuir* **10** 4367–73
[32] Tuteja A, Mackay M E, Hawker C J and Van Horn B 2006 *J. Polym. Sci. Polym. Phys. Edn* **44** 1930–47
[33] Tuteja A, Mackay M E, Hawker C J and Van Horn B 2005 *Macromolecules* **38** 8000–11
[34] de Gennes P G 1979 *C. R. Acad. Sci. Paris* B **288** 219–20
[35] BrochardWyart F, de Gennes P G, Hervert H and Redon C 1994 *Langmuir* **10** 1566–72
[36] Redon C, Brzoska J B and BrochardWyart F 1994 *Macromolecules* **27** 468–71
[37] Krishnan R S, Mackay M E, Duxbury P M, Pastor A, Hawker C J, Horn B V, Wong M S and Asokan S 2007 *Nano Lett.* **7** 484–9
[38] Hariharan A, Kumar S K and Russell T P 1993 *J. Chem. Phys.* **98** 4163–73
[39] Thompson R B, Ginzburg V V, Matsen M W and Balazs A C 2002 *Macromolecules* **35** 1060–71
[40] Seemann R, Herminghaus S and Jacobs K 2001 *Phys. Rev. Lett.* **86** 5534–7
[41] Parsegian V A 2005 *van der Waals Forces: A Handbook for Biologists, Chemists, Engineers, and Physicists* (Cambridge: Cambridge University Press)
[42] Ambekar R, Gupta V and Bogy D B 2005 *J. Trib-Trans. ASME* **127** 530–6
[43] Mackay M E, Dao T T, Tuteja A, Ho D L, Van Horn B, Kim H C and Hawker C J 2003 *Nat. Mater.* **2** 762–6
[44] Millan M D, Locklin J, Fulghum T, Baba A and Advincula R C 2005 *Polymer* **46** 5556–68
[45] Graessley W W and Edwards S F 1981 *Polymer* **22** 1329–34
[46] O'Hern C S, Silbert L E, Liu A J and Nagel S R 2003 *Phys. Rev.* E **68** 011306
[47] Lee S H, Yoo P J, Kwon S J and Lee H H 2004 *J. Chem. Phys.* **121** 4346–51
[48] Frischknecht A 2007 private communication